# Characterization of Cathode/Electrolyte Interphases for IT-SOFCs

L. Baqué[1,*], K. Padmasree[2], A. F. Fuentes[2], A. Serquis[1], A. Soldati[1]

[1]CONICET, CAB-CNEA, Av. Bustillo 9500, (8400) Bariloche, Argentina.
[2]Cinvestav Unidad Saltillo, Apartado Postal 663, Saltillo, México, 25000.
[*]Tel: +54294445100 Ext. 5383; e-mail: baquel@cab.cnea.gov.ar

## ABSTRACT

Solid oxide fuel cells (SOFCs) represent an efficient and environmental friendly technology for obtaining electrical power and heat. In recent years, a considerable research effort has been done in order to decrease their operation temperature from 800-1000ºC to the 500-800ºC range. However, the main drawback of lowering SOFC operating temperature is the reduction of cell performance and, hence, each individual component and their interfaces must be optimized. In this work, we studied symmetrical cells composed by high performance nanostructured $La_{0.4}Sr_{0.6}Co_{0.8}Fe_{0.2}O_3$ (LSCFO) cathodes deposited by spin coating on $Ce_{0.8}Y_{0.2}O_2$ (CYO) substrates. CYO electrolytes were synthesized by mechanical milling using two different milling times. Longer milling time produces electrolytes with smaller grain sizes, narrow size distribution and higher density. Bulk conductivity values are similar for both electrolytes, while grain boundary conductivity was slightly higher for the electrolyte prepared with shorter milling time. All this indicates that longer milling time does not improve electrolyte conductivity but, instead, it can have a detrimental effect.

*Keywords:* Solid Oxide Fuel Cells; Electrolyte; Interphase

## 1. Introduction

Solid oxide fuel cells (SOFCs) represent an efficient and environmental friendly technology to convert directly hydrogen and fossil fuels into electrical power and heat [1]. These devices require high operation temperature to allow the transport of oxygen ions through the ceramic components of the cell, challenging the long term stability and inducing rapid degradation of the cell. In recent years, a considerable research effort has been done in order to decrease the operation temperature from 800-1000ºC to the 500-800ºC range in the so-called Intermediate Temperature (IT)-SOFCs [2]. One of the materials of choice for IT-SOFCs electrolytes is the ceria based oxides because they present higher oxygen ion conductivities at lower operation temperatures.

SOFC electrolytes must be completely dense in order to avoid the contact between the oxygen fed on the cathode side with the hydrogen supplied at the anode side [1]. Ceria based oxides require high temperatures (up to 1600ºC) for achieving appropriate density. The use of mechanical milling during the synthesis of electrolyte powders allows obtaining uniform ultrafine non-agglomerated particles with high surface area that can be easily compacted and sintered as dense pellets [1,3,4]. In general, the electrolyte performance is evaluated by measuring its electrical conductivity. The use of the Electrochemical Impedance Spectroscopy (EIS) technique is useful to separate the bulk and the grain boundary contributions to electrolyte conductivity. However, these phenomena occurs at an unworkable frequency range and, hence, the accurate evaluation of electrolyte performance must be done at low temperatures. The main drawback of using intermediate temperatures is the increase of the cathode overpotential [5]. Therefore, expensive Pt electrodes (not suitable for practical SOFC operation) are generally used to evaluate the electrolyte performance.

It is also important to note that the performance of the whole cell depends not only of each individual component but also of the interphase between them [6,7]. Therefore, the use of real SOFC cathodes is important when evaluating electrolyte performance. This issue can be overcome with the use of nanostructured mixed conducting oxide cathodes, since these cathodes present considerably low overpotential especially at low temperatures [8,9].

In this work, we have studied symmetrical cells composed of high performance nanostructured $La_{0.4}Sr_{0.6}Co_{0.8}Fe_{0.2}O_{3-d}$ (LSCFO) cathodes deposited by spin coating on $Ce_{0.85}Y_{0.15}O_{2-d}$ (CYO) electrolytes. LSCFO cathodes were synthetized by an acetic acid based method, while the CYO electrolytes were synthesized by mechanical milling. The microstructure of the electrolytes, the cathodes and the cathode/electrolyte interphases was investigated by Scanning Electron Microscopy (SEM). The electrochemical performance of these assemblies was studied by EIS within the 100-600ºC temperature range under pure oxygen.

## 2. Experimental

$Ce_{0.85}Y_{0.15}O_{2-d}$ (CYO) powders were prepared by mechanical milling [3,4]. Stoichiometric mixtures of high purity (Aldrich, >99+%) $CeO_2$ and $Y_2O_3$ oxides were placed in zirconia containers together with 20 mm diameter zirconia balls as grinding media (balls to powder mass ratio = 10:1). Dry mechanical milling was carried out in air in a planetary ball mill by using a rotating disc speed of 350 rpm. Two milling times were used: 1h and 18 h. The obtained powders were uniaxially pressed with a pressure of 5 MPa to form pellets with ~10 mm diameter and ~1.4 mm thickness, and then sintered at 1500ºC for 5 h.

$La_{0.4}Sr_{0.6}Co_{0.8}Fe_{0.2}O_{3-d}$ (LSCFO) powders were synthetized by an acetic acid-based method. Detailed preparation procedure and microstructural characterization of these cathodes were reported elsewhere [6,8,9]. These powders were dispersed in an ink and deposited onto both sides of CYO substrates by the spin coating technique. Cathode covered completely the electrolyte surface with a geometric area of ~0.95 $cm^2$. Afterwards, these assemblies were heat treated at 900ºC, resulting in a symmetrical cell configuration used for electrochemical measurements. Two LSCFO/CYO/LSCFO cells were obtained: one prepared with CYO powder milled for 1h (from now on called CYO1h) and another one prepared with CYO powder milled for 18 h (from now on denoted as CYO18h).

Impedance measurements were performed in the 100-600ºC temperature range under pure oxygen. Impedance spectra were recorded using a potentiotast/impedance analyzer Autolab (Eco Chemie BV) within $10^{-3}$-$10^{6}$ Hz frequency range. A stabilization time of at least 3 h elapsed before each EIS measurement. Gold grids, slightly pressed on electrodes, were used as current collectors. Electrolyte and cathode microstructure was characterized by SEM.

## 3. Results and discussion

*3.1. Scanning electron microscopy*

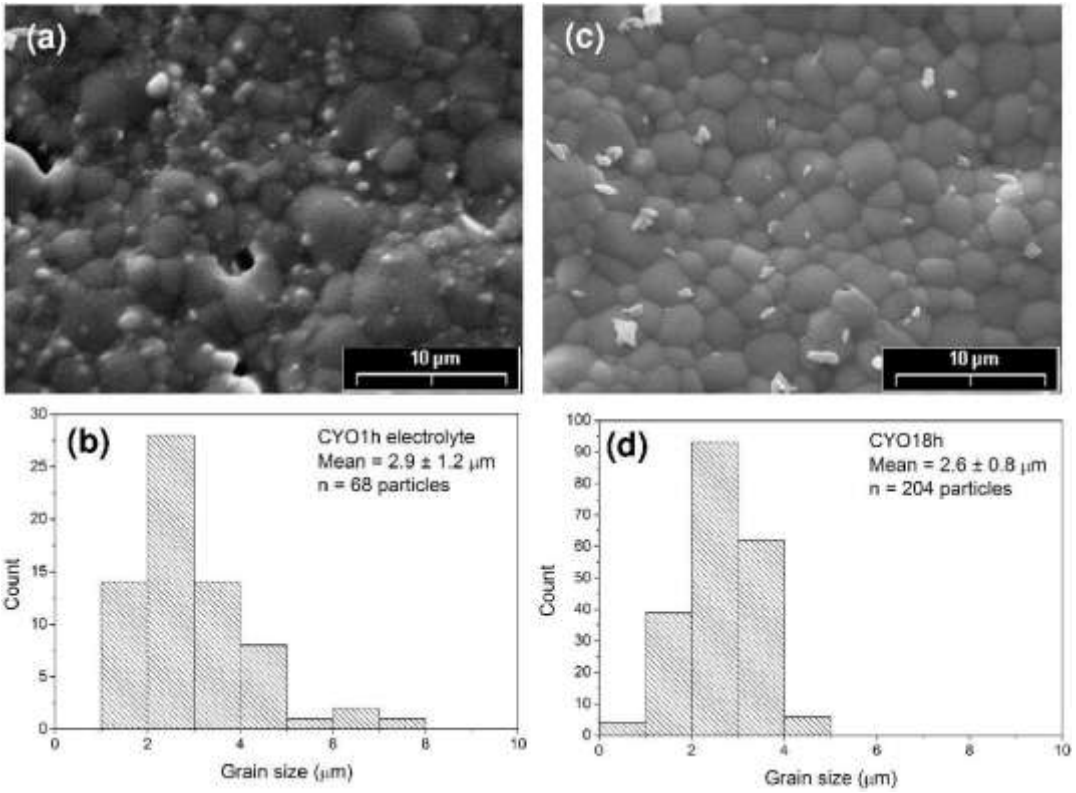


Fig 1. (a,c) SEM images and (b,d) grain size distributions of (a,b) CYO1h and (c,d) CYO18h electrolyte surfaces before cathode deposition.

SEM images from CYO1h and CYO18h electrolyte surfaces before cathode deposition are shown in Figures 1a and c, respectively. The corresponding grain size distribution is plotted in Figures 1b and d, respectively. Statistical analyses indicate that the CYO18h sample presents a smaller mean grain size with a narrow grain size distribution. All this is in agreement with the longer milling time used for preparing the starting powders of the CYO18h electrolyte.

Figure 2 displays SEM images from LSCFO/CYO1h/LSCFO and LSCFO/CYO18h/LSCFO cells after EIS measurements. Cathode surface is similar for both cells (see Figures 2a and b), showing some superficial cracks. It can be also observed that the cathode is composed of submicrometric particles. The thickness and porosity look also similar for both cathodes (see Figures 2c and d). Some closed pores of micrometric sizes can be observed in the CYO1h electrolyte cross-section (Figure 2c), while CYO18h appears fully dense Figure 2d). This suggests that the grain size distribution obtained by using 18 h milling time is more adequate for compacting the powders and sintering denser electrolyte pellets.

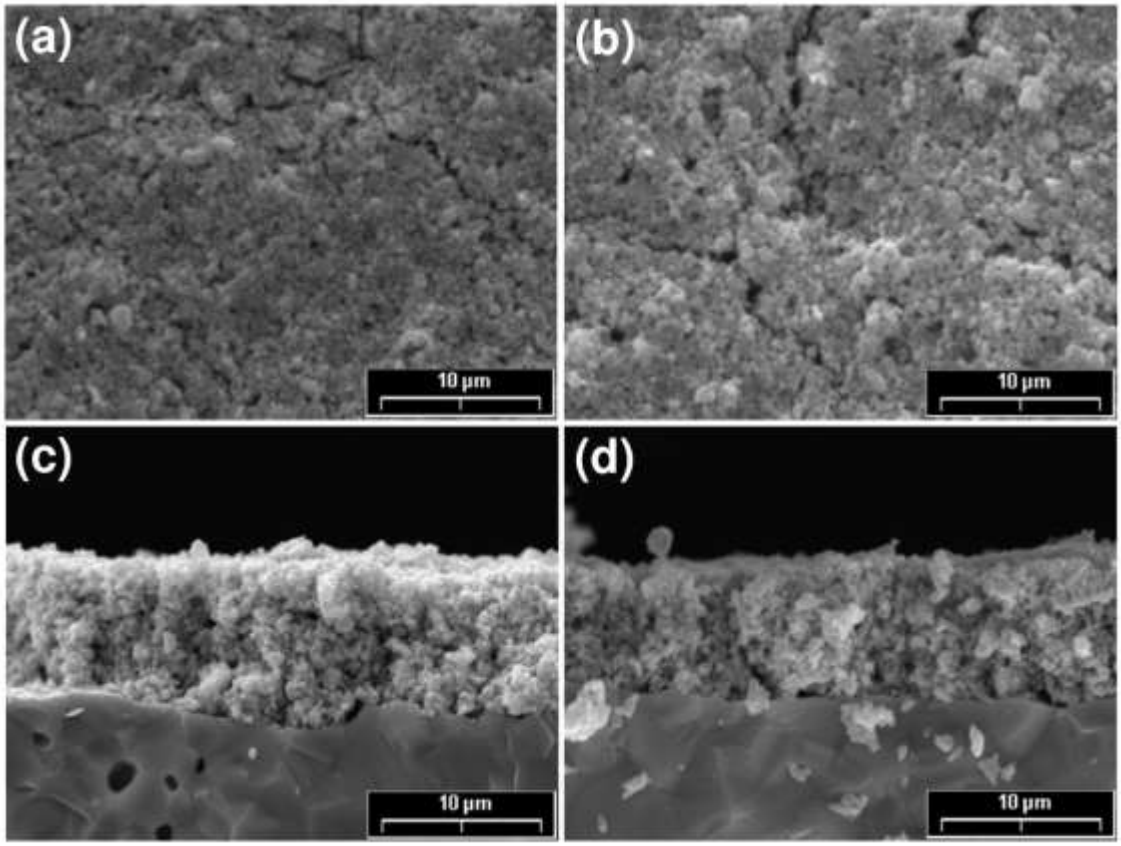


Fig 2. (a,b) Surface and (c,d) cross-section SEM images of (a,c) LSCFO/CYO1h/LSCFO and (b,d) LSCFO/CYO18h/LSCFO symmetrical cells after EIS measurements.

*3.2. Electrochemical impedance spectroscopy*

A typical impedance spectrum measured under pure oxygen at 250ºC corresponding to the LSCFO/CYO1h/LSCFO cell is shown in Figure 3. Part of an arc can be distinguished at the highest frequencies, a complete arc can be individualized at intermediate frequency, and a small part of a third arc can be observed at very low frequencies. These three contributions were observed for all the measured spectra and were fitted with the equivalent circuit displayed in the inset of Figure 3. The high frequency arc was fitted with a subcircuit composed of a resisitance ($R_B$) in parallel with a constant phase element ($CPE_B$), and represents the conduction through the electrolyte bulk. Similarly, the intermediate frequency contribution was fitted with the $R_{GB}$//$CPE_{GB}$ parallel subcircuit and represents the grain boundary conduction in the electrolyte. The low frequency contribution is related to the oxygen reduction reaction (ORR) at the cathode, including the oxygen ion transfer through the cathode/electrolyte interface. The real part of this later contribution ($R_{cathode}$) was determined with the procedure described in [9].

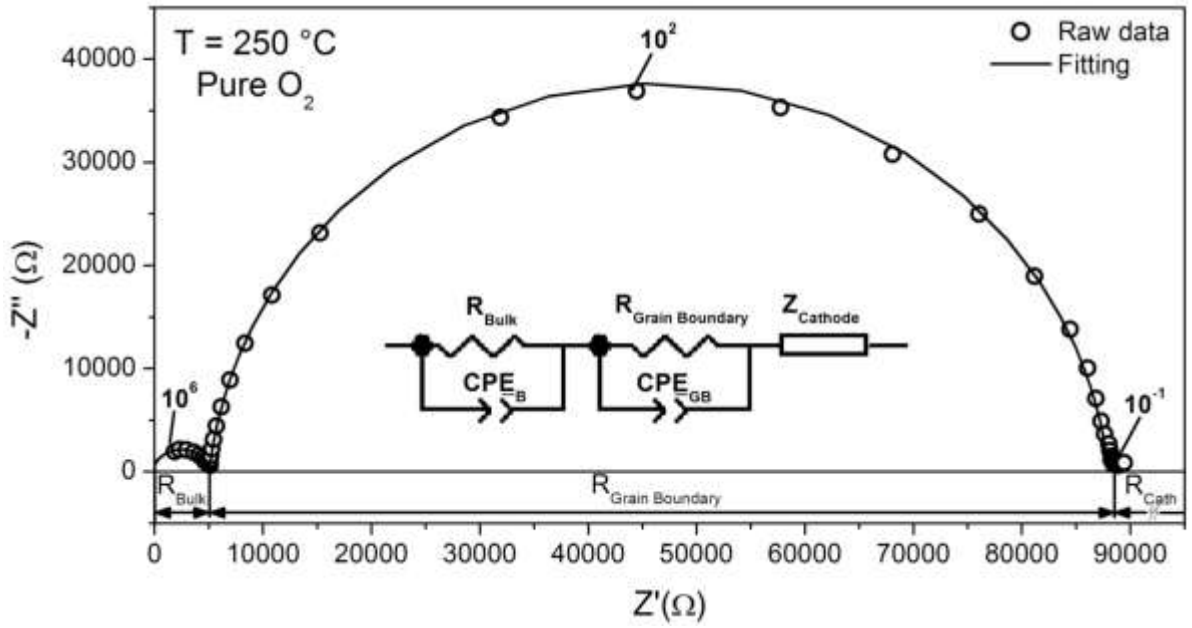


Fig 3. Nyquist plot of an EIS spectrum recorded under pure oxygen at 250°C for the LSCFO/CYO1h/LSCFO symmetrical cell. The numbers indicate the frequency in Hz. The inset shows the equivalent circuit used for fitting.

Electrolyte bulk and grain boundary conductivities can be estimated by using the equation:

$$\sigma_i = \frac{L}{R_i A} \qquad (1)$$

where $\sigma_i$ is the conductivity (bulk or grain boundary), $L$ is the electrolyte thickness, $R_i$ is the corresponding resistance (estimated by fitting the EIS spectra as described above), and $A$ is the geometric electrolyte area.

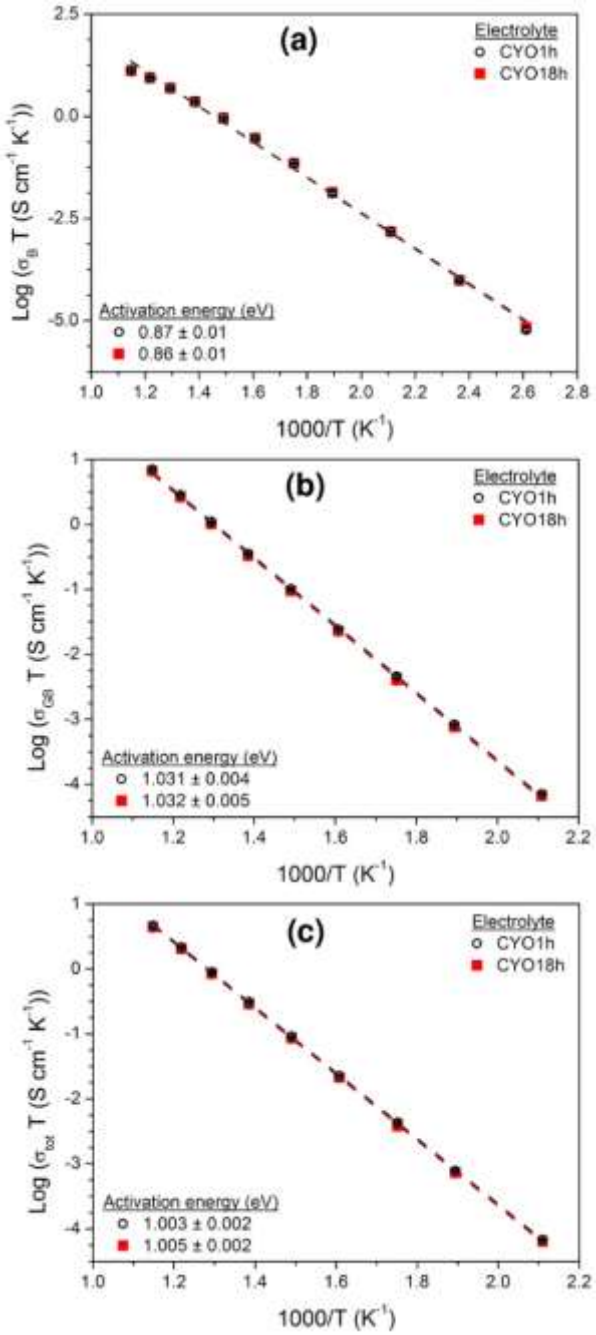


Fig 4. Arrhenius plots of (a) bulk, (b) grain boundary and (c) total conductivity values measured under pure oxygen corresponding to CYO1h and CYO18h electrolytes. The dotted lines represent the linear fitting of values.

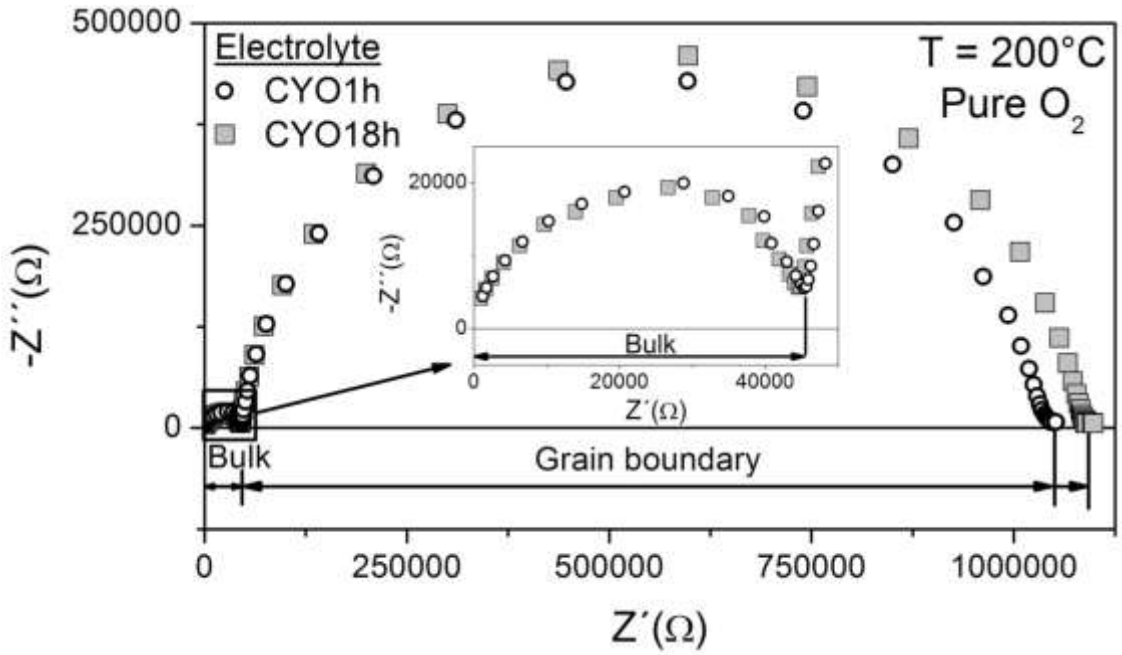


Fig 5. Nyquist plot comparing EIS spectra measured at 200°C under pure $O_2$ corresponding to CYO1h and CYO18h electrolytes. The inset shows a detail of the high frequency contribution.

Similarly, the total electrolyte conductivity can be estimated by using equation (1) with $R_{total}$ defined as the sum of $R_B$ and $R_{GB}$. Figure 4 shows the Arrhenius plots of the bulk, grain boundary and total conductivities of CYO electrolytes prepared with 1 h and 18 h milling time. Bulk conductivity values are practically the same for both electrolytes, while grain boundary conductivity is slightly higher (~ 5%) for the electrolyte prepared with 1 h milling time. Therefore, the conductivity values are also ~ 5% higher for the electrolyte prepared with 1 h milling time. This can be clearly observed in Figure 3, where two EIS spectra corresponding to CYO electrolytes prepared with 1h and 18 h milling time are compared. Spectra displayed in Figure 5 were measured at 200°C in pure oxygen but similar results were observed over the entire temperature range.

According to the SEM imaging analysis presented in the previous section, CYO18h electrolyte has slightly smaller grain sizes. It is a priori expected that electrolytes with smaller grain sizes exhibit higher grain boundary conduction. This is because they contain more grain boundaries and grain boundary conduction is, in principle, faster than in bulk [10]. Nonetheless, CYO18h electrolyte presents conductivity values that are 5% lower than those of the CYO1h electrolyte. Several factors can negatively influence grain boundary conduction. A typical example is the presence of impurities that tend to segregate at grain boundary hindering the conduction [11]. In order to elucidate this issue, a study of the composition in the electrolyte grain boundaries is planned in the near future.

Cathode area specific resistance ($ASR_{cathode}$) values were evaluated by using the following equation:

$$ASR_{cathode} = R_{cathode}A \qquad (2)$$

$ASR_{cathode}$ values are plotted in Figure 6. LSCFO/CY1h/LSCFO cell shows $ASR_{cathode}$ values about 1.3-1.9 times higher than those corresponding to the LSCFO/CYO18h/LSCFO cell. However, some scatter within $ASR_{cathode}$ values corresponding to the same cathode can be observed. This scattering can be produced by two factors. The first one is the fact that there is some overlap between the electrolyte grain boundary contribution and the cathode contribution, especially at high temperature. In addition, the $R_{cathode}$ values are more than one order of magnitude lower than the total electrolyte resistance ($R_{total}$) values. Consequently, the estimation of $ASR_{cathode}$ is cumbersome yielding to some errors. The second factor is the apparent inherent scatter found in *ASR* values of cathodes deposited in the identical conditions by spin coating. Variations in *ASR* values up to a factor of 3 were previously reported [8]. All this indicate that the differences in $ASR_{cathode}$ values observed in Figure 6 are within the expected ones for these cathodes and they do not necessarily mean a difference between cathode microstructures and or cathode/electrolyte interphases.

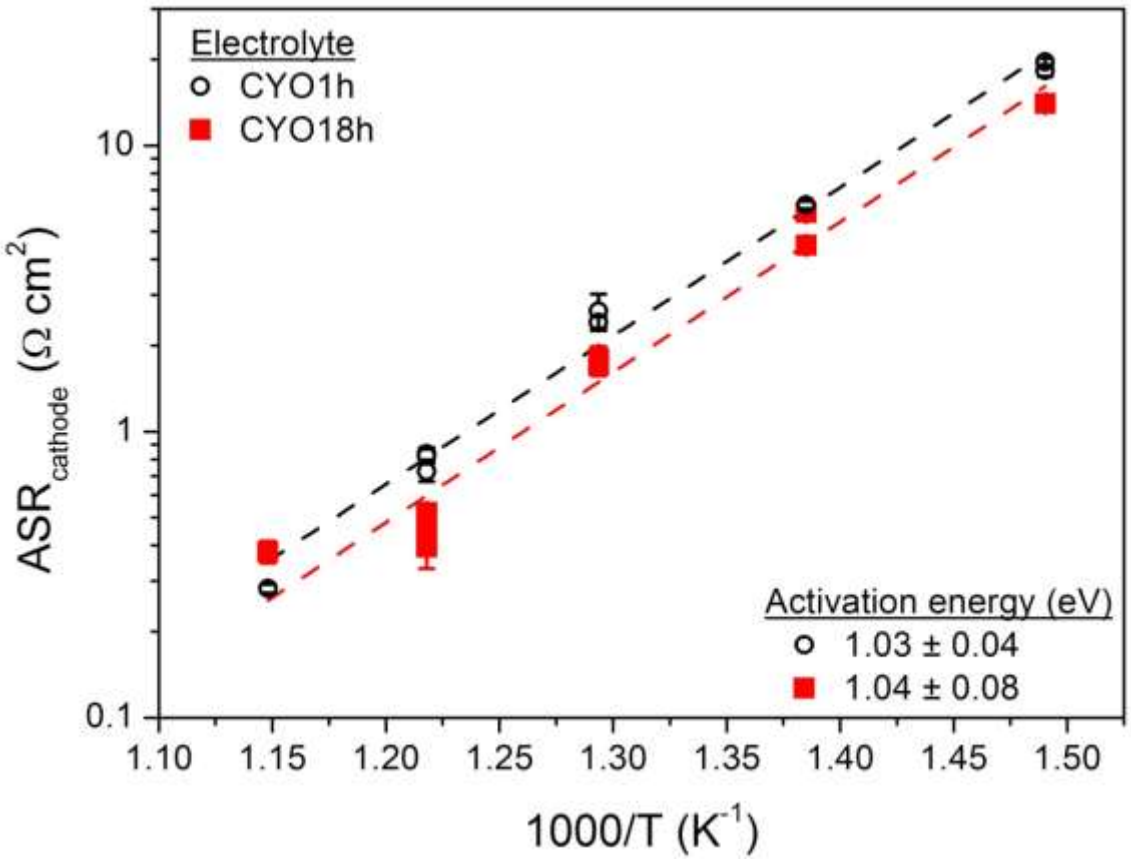


Fig 3. Nyquist plot comparing EIS spectra measured at 200°C under pure $O_2$ corresponding to CYO1h and CYO18h electrolytes. The dotted lines represent the linear fitting of values.

## 4. Summary and perspectives

The electrochemical and microstructural properties of LSCF/CYO/LSCFO symmetrical cells were evaluated. CYO electrolytes were prepared by mechanical milling using two different milling times: 1h and 18 h. CYO electrolyte prepared with longer milling time exhibits somewhat smaller grain sizes, a narrow size distribution, and a higher density. Bulk conductivity is similar for both electrolytes while grain boundary and total conductivities are ~5% higher for the electrolyte prepared with 1 h milling time. This indicates that increasing milling time does not improve electrolyte performance but, on the contrary, it can even have a detrimental effect on it.

## Acknowledgements

This work is part of a bilateral collaboration project funded by CONICET-Argentina and CONACYT-Mexico (Funding D1765). This research effort was also funded by University of Cuyo, CNEA and ANPCyT-PICT (Argentina).

## References

[1] N. Minh, Ceramic fuel cells. J. Am. Ceram. Soc. 1993; 76: 563-588.

[2] B. C. H. Steele, A. Heinzel, Materials for fuel-cell technologies. Nature 2001; 414:345-352.

[3] K. P. Padmasree, R. A. Montalvo-Lozano, S. M. Montemayor, A. F. Fuentes, Electrical conduction and electric relaxation process in $Ce_{0.8}Y_{0.2}O_{1.9}$ electrolyte system. J. Alloys Compd. 2011; 509: 8584–8589

[4] R. A. Montalvo-Lozano, S. M. Montemayor, K. P. Padmasree, A. F. Fuentes, Effect of $Ca^{2+}$ and $Mg^{2+}$ additions on the electrical properties of yttria doped ceria electrolyte system. J. Alloys Compd. 2012; 525: 184-190.

[5] E. Ivers-Tiffée, A. Weber, D. Herbstritt, Materials and technologies for SOFC components. J. Eur. Ceram. Soc. 2001; 21: 1805-1811.

[6] A. Soldati, L. Baqué, H. Troiani, C. Cotaro, A. Schreiber, A. Caneiro, A. Serquis, High resolution FIB-TEM and FIB-SEM characterization of electrode/electrolyte interfaces in solid oxide fuel cells materials. Int. J. Hydrogen Energy 2011; 36: 9180-9188.

[7] A. Montenegro-Hernández, A. Soldati, L. Mogni, H. Troiani, A. Schreiber, F. Soldera, A. Caneiro, Reactivity at the $Ln_2NiO_{4+\delta}$/electrolyte interphase (Ln = La,Nd) studied by electrochemical impedance spectroscopy and transmission electron microscopy. J. Power Sources 2014; 265: 6-13.

[8] L. Baqué, A. Caneiro, M. S. Moreno, A. Serquis, High performance nanostructured IT-SOFC cathodes prepared by novel chemical method. Electrochem. Commun. 2008; 10: 1905-1908.

[9] L. Baqué, E. Djurado, C. Rossignol, D. Marinha, A. Caneiro, A. Serquis, Electrochemical performance of nanostructured IT-SOFC cathodes with different morphologies. ECS Trans. 2009; 25: 2473-2480.

[10] P. Heitjans, S. Indris, Diffusion and ionic conduction in nanocrystalline ceramics. J. Phys.: Condens. Matter. 2003; 15: R1257.

[11] T. S: Zhang, J. Ma, H. Cheng, S. H. Chan, Ionic conductivity of high-purity Gd-doped ceria solid solutions. Mater. Res. Bull. 2006; 41: 563-568.